

Robust Automated Void Detection in Solder Balls and Joints

Asaad F. Said¹, Bonnie L. Bennett², Lina J. Karam¹, and Jeff Pettinato²

¹School of Electrical, Computer, & Energy Engineering, Arizona State University, Tempe, AZ, USA

²Intel Corporation, USA

asaad.said@asu.edu, bonnie.l.bennett@intel.com, karam@asu.edu, jeffrey.s.pettinato@intel.com

Abstract

Accuracy in solder balls and joint void detection is very important. If voids are incorrectly identified, board yield will be affected by incorrect scrapping and rework. Voids are difficult to detect using manual inspection alone. One current solution to make voids visible involves the use of a 2D x-ray system to image the boards. Some existing x-ray inspection systems have void detection algorithms that require the use of intensive, time consuming, fine tuning operations. These algorithms typically use two different global thresholds to segment the balls or joints and the voids using operator trial and error. However, using global thresholding over the entire image is invalidated due to varying image brightness. Existing methods also eliminate balls or joints that are partially occluded by other components due to difficulties in segmentation. The results are that many voids that can be easily observed by the human eye are missed by the existing automated methods.

In this paper, a robust, accurate, and automatic void detection algorithm is proposed. The method is applicable to either Pre SMT solder balls or post SMT solder joints. For simplicity, the term balls will be used throughout the document. The proposed method is able to detect voids with different sizes inside the solder balls, including the ones that are occluded by board components and under different brightness conditions. The proposed method consists of segmenting individual balls, extracting occluded balls, and segmenting voids inside the solder balls. The segmentation of the individual balls is achieved by using the proposed histogram and morphological based segmentation method. A voting procedure is used to segment the occluded balls where the pixels inside the occluded area are checked to obtain candidate pixels representing the occluded joint's or ball's centroids. An independent edge detection procedure is used to get candidate voids inside individual balls. Mathematical morphology operations are used to locate all possible valid voids and remove non-void areas. The proposed algorithm was applied to 3 different Intel products. The results of the proposed method were compared to the results obtained by an automated algorithm in an existing state-of-the-art 2D x-ray inspection system, the results obtained by trained operators from 2D x-ray images, and the results obtained by trained operators from 3D CT scan images. The results (pre SMT solder balls) show that the proposed method is capable of successfully locating all possible visible voids inside the solder ball even the ones that were missed by using other methods as well as those that are hard to see by the human eye. The results also show a high correlation with ground-truth data obtained from 3D CT scan and experienced operators. The algorithm is fully automated, benefits the manufacturing process by reducing operator effort and provides a cost effective solution to improve output quality.

1. Introduction

Voids are one of the major defects in solder balls and joints and are defined as cavities formed inside the solder joint due to the amount of out-gassing flux that gets entrapped in the solder joint during reflow. Some causes of voids are trapped flux that has not had enough time to be released from the solder paste, and contaminants on improperly cleaned circuit boards. Voids in solder balls and joints are also caused by the reduction or metallic oxides by the soldering fluxes [1]. Voids appear as a lighter area inside the solder balls and joints on a 2D x-ray image and are typically found randomly throughout the package [2]. Previous studies show that the existence of voids decreases the solder joint life validated through mechanical testing and thermal cycle testing [3]. In [4], the authors concluded that smaller voids grow much more slowly than the bigger voids. The extensive use of solder balls and joints on printed circuit boards (PCB) necessitates reliable, void detection in the balls and joints to prevent infant mortality failures. The Institute for Printed Circuits (IPC) and the Joint Electron Device Engineering Council (JEDEC) have developed standards for inspecting assemblies of electronic products. IPCA610D specifies a 25% or less cumulative voiding percentage in post SMT solder joints. JEDEC void inspection criteria are based on the size of the void and the cumulative percentage of voiding in an individual ball. A new JEDEC guideline for void inspection criteria is in preparation by the JC14-1 committee.

A solder ball has a spherical shape as shown in Fig.1(a). Voids are distributed randomly inside the solder ball as shown in Fig. 1(b) which gives a cross-sectional view inside the spherical solder ball. The 2D top view of the spherical solder ball is shown in Fig.1(c). Voids are hard to locate inside solder balls and joints using manual inspection tools. 2D x-ray machines are used to make the voids inside the solder balls and joints visible to the operator as shown in Fig. 2. The output of the x-ray machine is shown in Figs. 2(a)-(d) which represents the 2D images of different products. Figs. 2(e)-(h) show a zoomed image

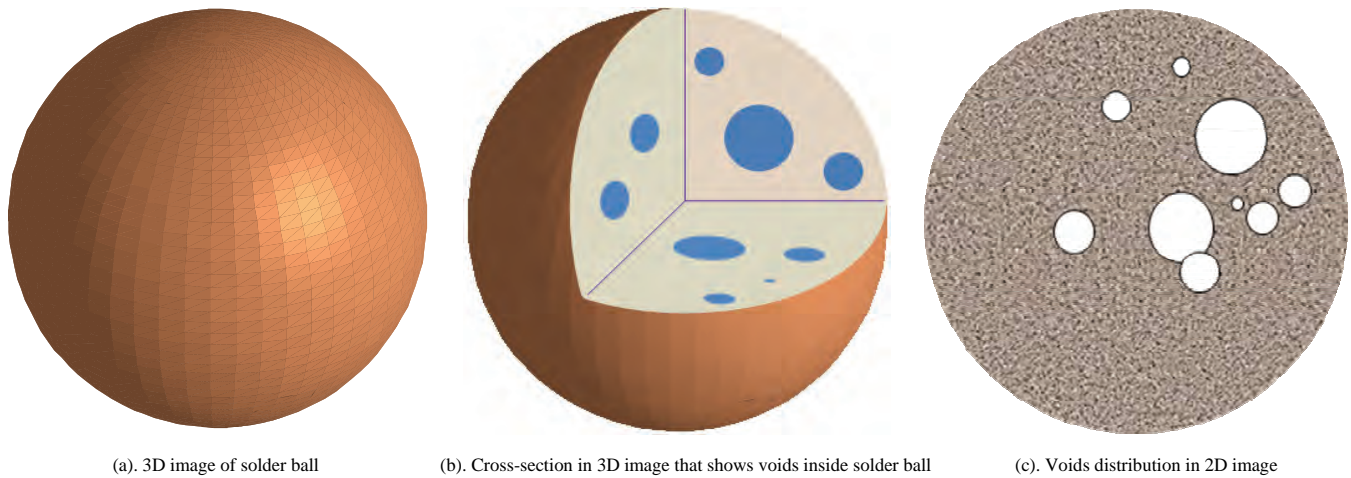


Fig.1: Solder ball shape in 3D and the distribution of voids in both 3D and 2D images.

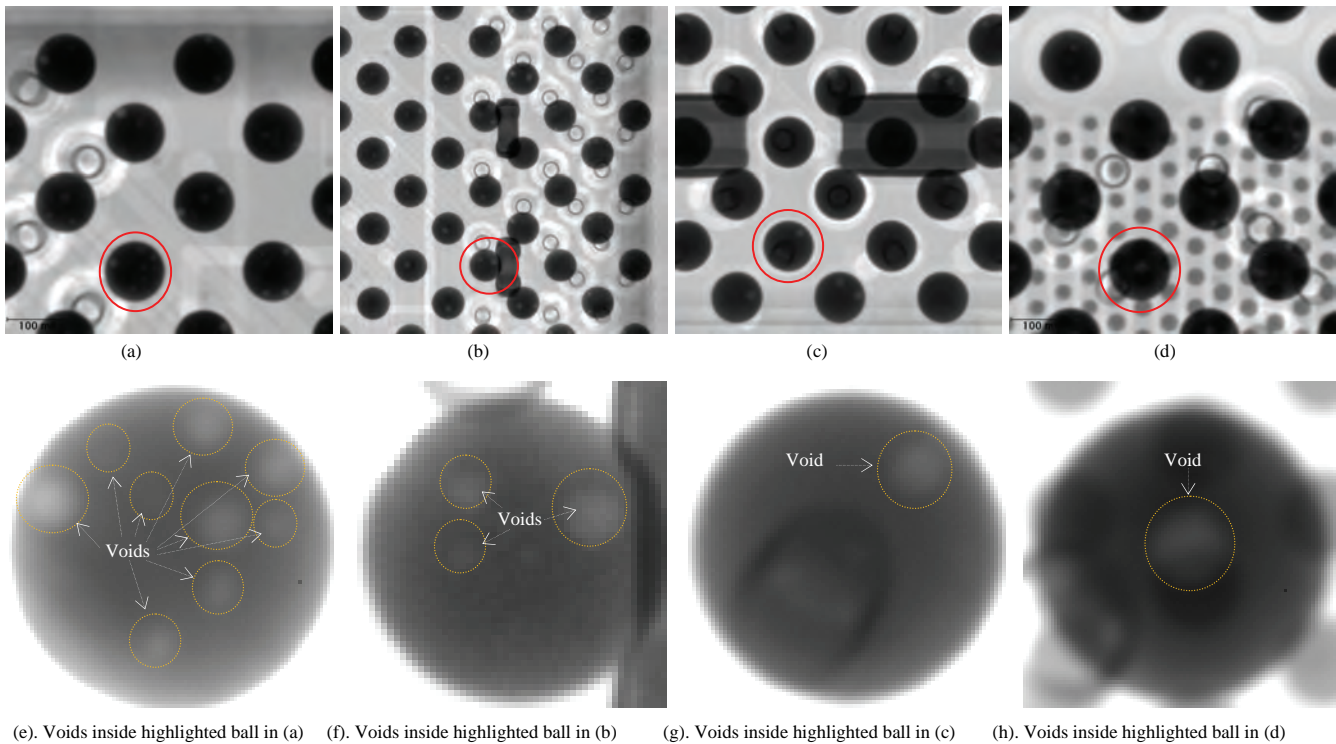


Fig.2: Example of 2D x-ray images that show voids inside solder balls in different product lines.

for balls that are highlighted in Figs. 2(a)-(d), respectively. The images in Figs. 2(e)-(h) are enhanced for visual clarity to show all possible voids inside the highlighted solder balls in Figs. 2(a)-(d). One of the methods used to locate voids inside solder balls is to use existing image enhancement software to examine the x-ray images manually after changing the image brightness and contrast. The operator must then detect and measure each observed void manually. A skilled operator takes around 4 minutes to locate and measure one void inside a solder ball which makes the manual process very tedious and time consuming. The process is also highly variable due to the difference in training, skill and other human characteristics of operators.

The necessity of getting a robust and reliable automated void detection algorithm is important. Before discussing existing void detection methods let us address the main challenges that are observed in the acquired 2D x-ray images. These challenges can be summarized as follows: (i).poor image contrast at some balls that make the voids difficult to detect by the human eye; (ii).interference of other components in the unit such as void-like artifacts, die bonds, vias (plated through holes), and overshadowing capacitors; (iii).irregular shapes (non-circular) caused by the fact that there can be overlapped voids

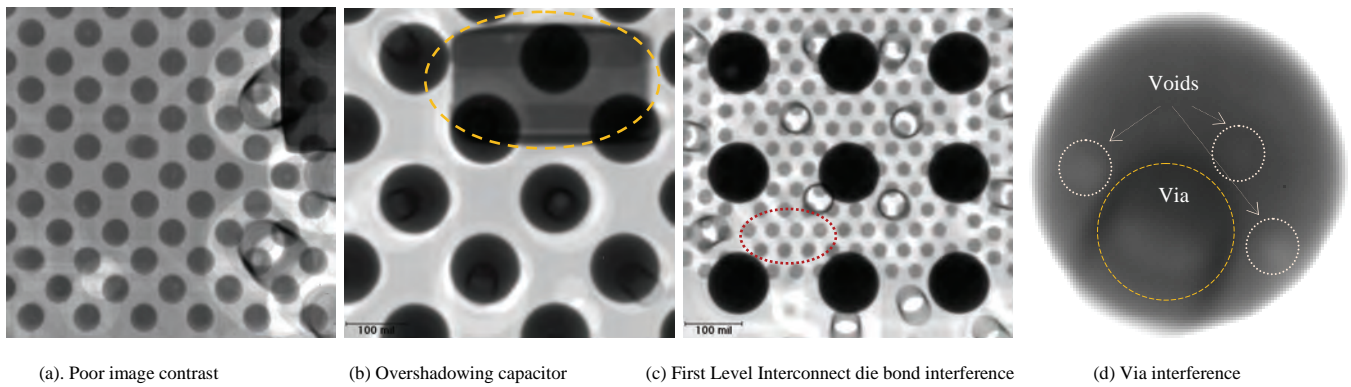


Fig. 3: Examples of some Challenges in the 2D x-ray images.

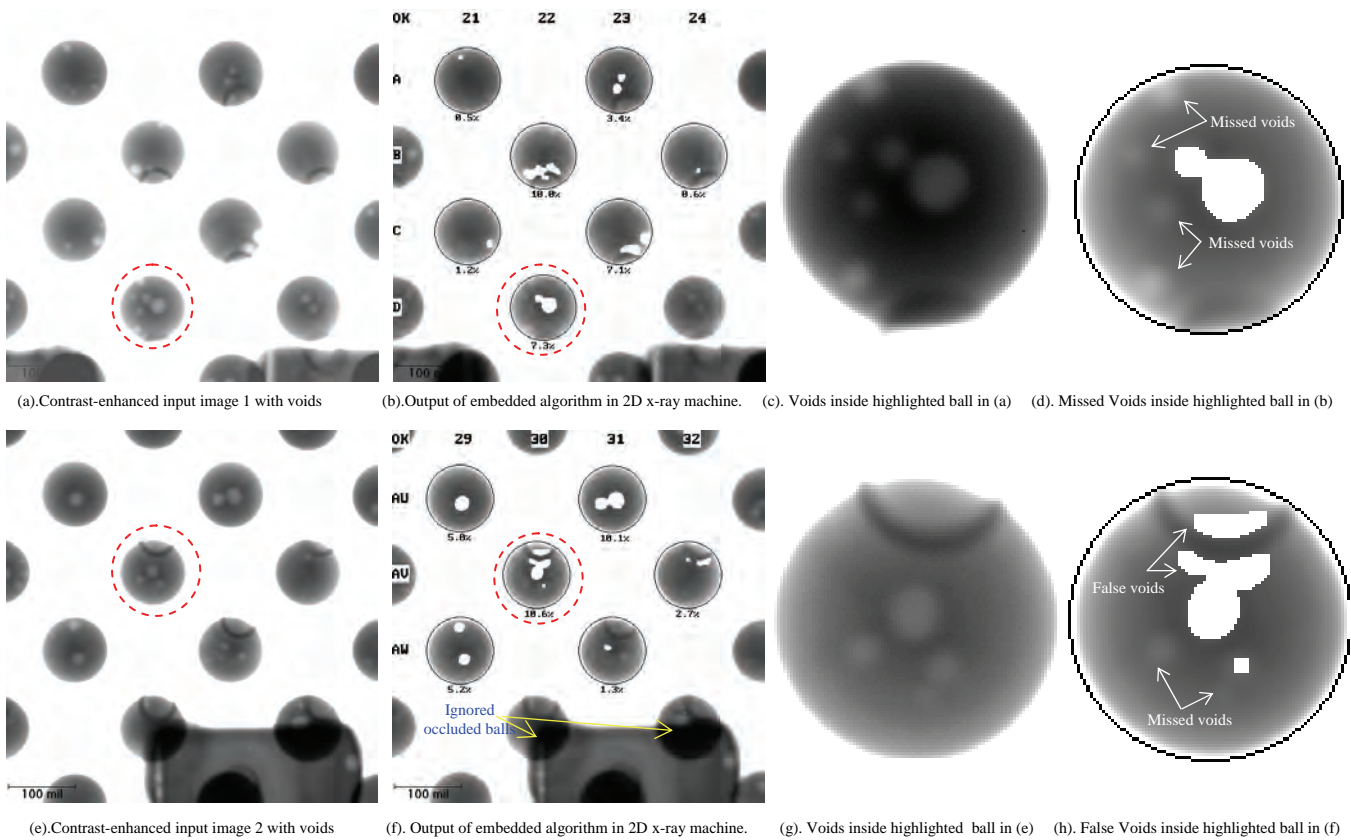


Fig.4: Results using 2D x-ray machine with an embedded void detection algorithm.

present in 2D images that do not conform to the predominant circular void shape; (iii). missing or overlapped voids not visible in the 2D x-ray images compared to the details obtained from the 3D CT scan images. Fig. 3 shows some examples of the aforementioned challenges in the 2D x-ray images. Most of the existing void detection systems do not provide solutions to tackle these issues which result in missed and false called voids and thus inaccurate detection.

Using a 2D x-ray machine is much faster and less expensive to measure each ball as compared to a 3D or multi-dimensional x-ray machine, but at a loss of some accuracy as mentioned above. Some existing 2D x-ray machines have embedded inspection systems that include void detection algorithms. However, the existing void detection algorithms that are used in 2D x-ray machines require intensive preprocessing steps and manual fine tuning. An example of the steps of image acquisition and void detection in 2D x-ray machine with an embedded void detection algorithm are as follows:

- The first step is to set up the 2D x-ray machine to make sure that there is visible gray scale difference between the solder balls, background and voids. The operator manually uses different gray scale levels for solder ball, background and voids depending on the intensity of the void level. The setting of the gray scale level is achieved by changing the current and voltage of the x-ray beam.
- The second step is to set up the void detection software. A typical software setup includes defining the expected solder ball size and additional inspection features. Some of these features can include segmentation threshold values such as the

threshold to identify the gray scale difference between a solder ball and background area, and the threshold to identify the difference between voids and solder ball. Threshold values are determined by the operator by trial and error. After using the selected threshold to segment the solder ball from the background, some feature parameters such as predefined size (area) of a solder ball are used to decide which one of the segmented regions should be processed and which one should be ignored. A global thresholding method cannot be optimized to provide sufficient adjustment to capture all voids with the lighting variations typically encountered in an x-ray image. In addition, this method is unable to segment the balls that are occluded by overshadowing components.

- The third step involves detecting the voids in the considered set of images using the software with the selected threshold values and inspection features.

An example of void detection using the above system is shown in Fig.4. The results shown in Fig.4 show that the 2D x-ray machine with an embedded void detection algorithm misses voids, detects many false voids and fails to process balls that are occluded by overshadowing capacitors. The system is also troubled by vias under the balls and classifies the vias as voids. In addition, this system requires a lot of manual operations and parameter tuning for each new product line.

This paper is organized as follows. Section 2 presents the steps of the proposed void detection algorithm. Performance results and comparison with existing methods are presented in Section 3. A conclusion is provided in Section 4.

2. Automated Void Detection Method

The main goal in this paper is to provide a reliable, highly accurate, and fully automated scheme for void detection in 2D x-ray images. The proposed algorithm is designed to be robust to the challenges that are present when dealing with 2D x-ray images as discussed in Section 1. In this section, we present more details about the proposed void detection algorithm which is capable of detecting voids with different sizes inside the solder balls and under different brightness conditions.

Fig. 5 shows the block diagram of the proposed automated void detection method. The block diagram summarizes the steps of the proposed method including solder ball segmentation, the extraction of solder balls that are occluded by overshadowing capacitors, the extraction of candidate regions inside each segmented solder ball, the selection of feature parameters, and the classification of the candidate regions inside the solder ball in order to exclude all non-void regions. Fig. 6 illustrates the steps of the proposed method. More details about the individual solder ball segmentation and the candidate void detection and classification are given in the following subsections.

2.1. Individual Solder Ball Segmentation

Due to the fact that the 2D x-ray images suffer from inconsistent lighting, in order to segment the solder ball area, it is important to use an adaptive threshold value which is based on the image intensity distribution instead of using a fixed threshold value. In the proposed method, an automatic thresholding value based on the image histogram analysis is applied to the original image to segment the solder balls. Fig. 6(b) shows the histogram of the 2D x-ray image shown in Fig. 6(a) where the histogram contains two main cluster regions represented by two distinct peaks: the solder ball and background regions. In order to segment the solder balls regions (ROIs) from the background region, the segmentation threshold is determined automatically based on the distribution (histogram) of the considered image. From the distribution of the input image, the mean of the image is computed and is used as the initial segmentation threshold value. The distribution range is then divided into two parts, also referred to as clusters, corresponding to pixel values below and above the current threshold, respectively. The threshold value is efficiently refined by computing the cluster means directly from the input image distribution without the need to segment the image. The updated threshold estimate is set to be the average of the two cluster means. This refinement step is repeated until the two cluster mean values no longer change, resulting in the final threshold estimate. This procedure converges in an average of 4 to 6 iterations. Fig. 6(c) shows the results after applying the above adaptive segmentation threshold computation procedure. Incomplete balls that are touching the image border are excluded from further void location processing. The removal of those incomplete balls is achieved by comparing each incomplete ball's area (A_i) with respect to the area of the individual complete ball (A_b), where A_b is taking as the median area of the segmented regions' areas inside the input image. Fig. 6(d) shows the results of excluding incomplete balls that are touching the image border and have an incomplete ball area less than 0.7 of the individual complete ball area (A_b).

Previous methods such as embedded algorithms in x-ray machines are unable to process balls that are occluded by overshadowing components, even though some of these balls may have high void percentages. In the proposed method, a voting procedure is devised to extract the occluded balls by locating their centroids. This can be achieved by exploiting the

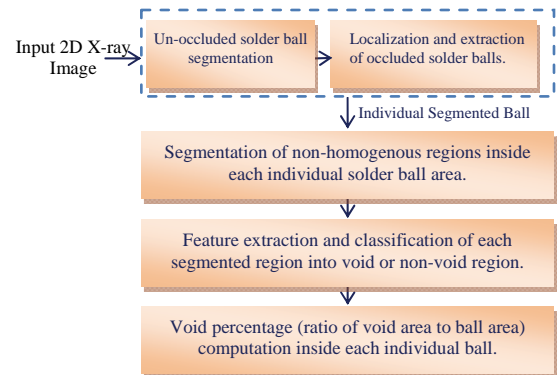


Fig 5. Block diagram of the proposed method for void detection inside solder balls.

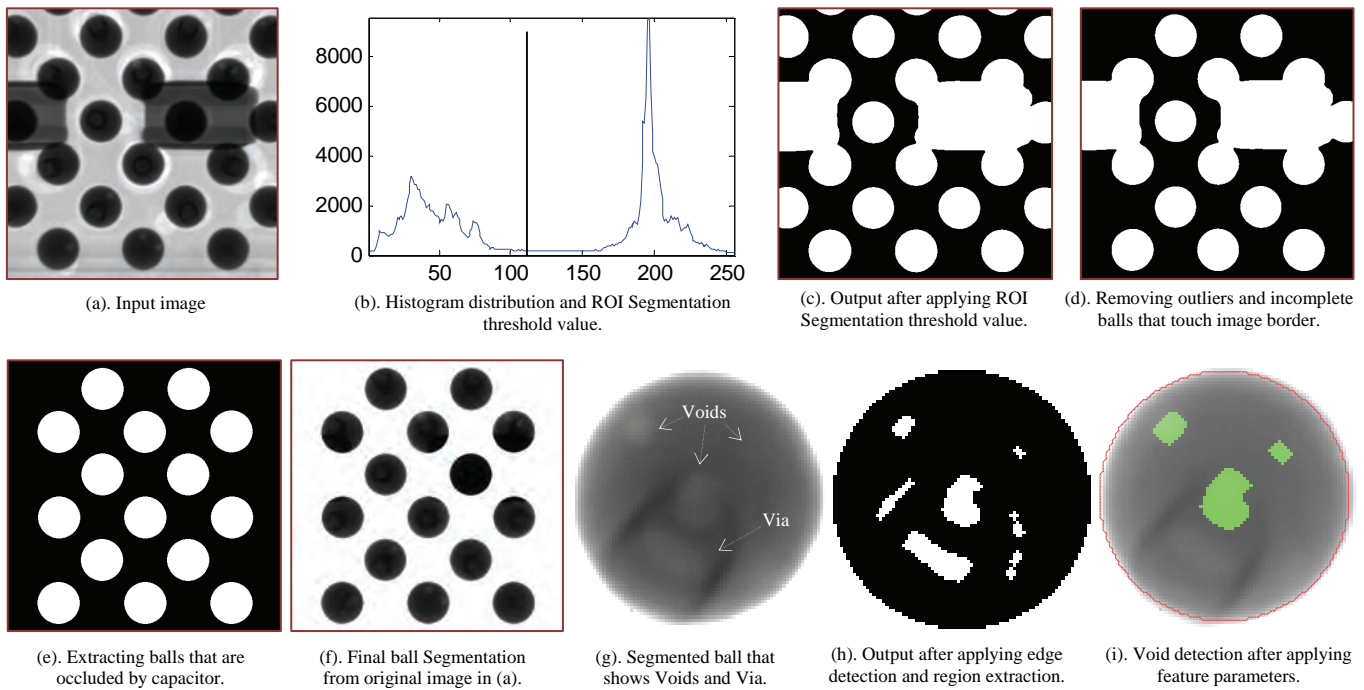


Fig. 6. Steps of the proposed void detection method.

fact that the solder balls are aligned along different directions, including 0° , $\pm 45^\circ$, $\pm 90^\circ$ as shown in the input image in Fig. 6(a). The extraction of the occluded balls' centroids using the proposed voting procedure is done as follows: (i). locate the occluded regions as the segmented regions whose area is greater than 1.2 of the individual ball's area A_b ; (ii). calculate the centroids of the individual complete balls outside the occluded regions; (iii). check the alignment of each pixel inside the occluded region in the directions of 0° , $\pm 45^\circ$, $\pm 90^\circ$ with respect to individual balls' centroids outside the occluded region; (iv). keep only those pixels that match at least two directions inside the occluded region; The results of this step produce isolated regions consisting of clusters of connected pixels, (v). calculate the centroid of each region using an image labeling procedure [5]; (vi). extract each occluded ball by drawing a circle centered at that extracted centroid with a radius $R = \sqrt{A_b/\pi}$, where A_b is the previously determined complete solder ball area, (vii). remove any false centroids by checking the distance between neighboring balls' centroids (remove if distance is less than 1.2 of the individual ball's diameter). The result of the proposed scheme after locating the occluded balls is shown in Fig. 6(e) which represents the final segmentation mask. Using the final segmentation mask, one can easily extract each individual complete ball from the original input image including the balls occluded by overshadowing capacitors as shown in Fig. 6(f).

2.2. Feature Extraction and Void Detection

Locating voids inside each segmented solder ball requires a robust classification procedure to detect actual voids and remove non-void regions. There are many challenges when it comes to automatically detecting actual voids and excluding non-void regions inside solder balls such as: lighting variation, die balls and via interference. It is thus important to process each individual ball independently to locate voids. This is needed in order to tackle the lighting variation and die ball interference issues. In the proposed scheme, each ball is extracted and treated independently by using an image labeling procedure [5]. To locate the contours of all possible regions inside the segmented solder ball for further processing, an edge detection procedure [6-11] is applied to the segmented solder ball. In our implementation, a simple Laplacian of Gaussian (LoG) edge detection method was found to produce accurate results [10-12]. The edge detection output can however result in some open contours. Closed contours are obtained by applying a morphological dilation operation [5, 13] using a structuring element of size 1. Each area inside a closed contour is then extracted by using an image labeling procedure [5]. Fig. 6(h) shows the results of edge detection and region extraction for the ball shown in Fig. 6(g). Each extracted region inside the solder ball should be classified as a void or non-void region. However, some artifacts (such as vias and die bonds) have void-like properties. Therefore, the devised classification method should be robust to such artifacts in order to detect actual voids and exclude suspect voids. For this purpose, the proposed automated classification method makes use of feature parameters that well describe the actual voids and are robust to artifacts such as vias and other interferences in the segmented ball. The employed features exploit the following properties of the void region: (i). voids are brighter compared to surrounding area (some vias are brighter as shown in Fig. 6(g)); (ii). voids have shapes close to a circular shape (can have irregular shape if the 2D image has overlapped voids). Consequently, the proposed feature parameters that are used for classification consist of an adaptive and automated classification threshold which is adaptively determined based on the brightness of each region and its

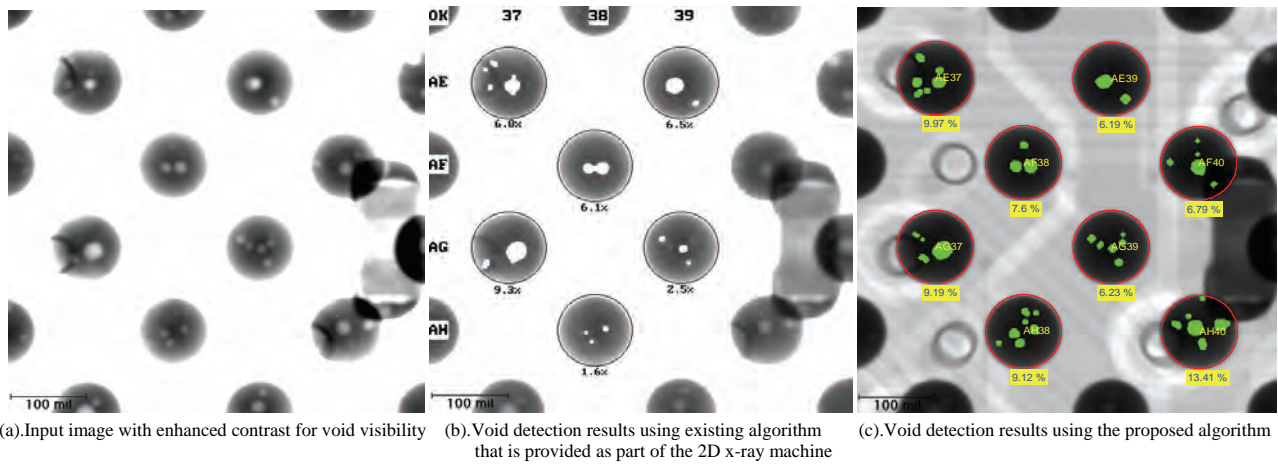


Fig. 7. Comparison between existing void detection algorithm in 2D x-ray machine and proposed void detection algorithm in product line B.

surrounding contour, and which can be used to remove non-void regions, and of a compactness factor [6] which can be used to exclude region with irregular shapes. The compactness factor of a considered segmented region is computed as $CF_i = p_i^2 / 4 \pi A_i$, where p_i and A_i represent the perimeter and the area of the considered region. If the region has a shape close to a circular shape, its compactness factor is close to “1”, otherwise it’s larger.

The proposed classification consists of 3 main stages: (i) the first stage is used to keep all candidate regions with void-like characteristics by using the aforementioned adaptive classification threshold and a large compactness factor filter; (ii). the second stage is used to refine the results of the first stage and eliminate more non-void regions (false calls) by using adaptive dilation to obtain a regulated shape followed by a smaller compactness factor filter (dilation removes small gaps inside the void that cause small shape irregularities); (iii). the third stage is used to remove vias while keeping all possible voids by using two feature parameters that are based on the area and the principal axis ratio of the segmented region. Fig. 6(h) shows all detected void and non-void regions inside the solder ball of Fig. 6(g) before applying the proposed classification procedure, while Fig. 6(i) shows the resulting detected voids inside the solder ball of Fig. 6(g) after using the proposed classification method.

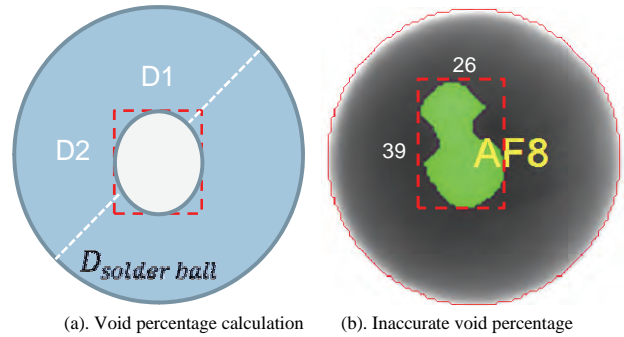


Fig.8. Manual void percentage calculation

3. Simulation Results

The proposed method was applied to different Intel product lines: A, B, and C. Each one of these product lines has different challenges in addition to die bond interference and inconsistent lighting such as: (i). product line A has limited via interference, and has a low void density per ball, (ii). product line B has limited via interference, and has a high void density per ball, and (iii).product line C has more via interference and medium void density per ball. The results of the proposed algorithm were compared to the results obtained from the existing latest 2D x-ray void detection algorithms that are provided as part of the x-ray imaging machine, the results obtained from 2D x-ray images by a trained operator, and the results obtained from 3D CT scan x-ray images which represents ground truth data.

3.1. Comparison with the data obtained from 2D X-ray embedded algorithm

The existing void detection algorithm in the 2D x-ray machine was applied to the three Intel products lines: A, B, and C. The performance of the algorithm shows satisfactory results in product line A, unsatisfactory results in product line B and produces a complete failure for product line C. Fig. 7 shows an example that illustrates the performance results of product line B for both the proposed method and the existing embedded algorithm that is provided with the 2D x-ray machine. From Fig. 7(b), it can be clearly seen that the existing embedded void detection algorithm produces false voids, misses a lot of voids, and does not process balls occluded by overshadowing components. In comparison, Fig. 7(c) shows that the proposed method outperforms the existing embedded void detection algorithm of the 2D x-ray machine and is able to detect voids in the occluded balls in addition to the ones in the non-occluded balls.

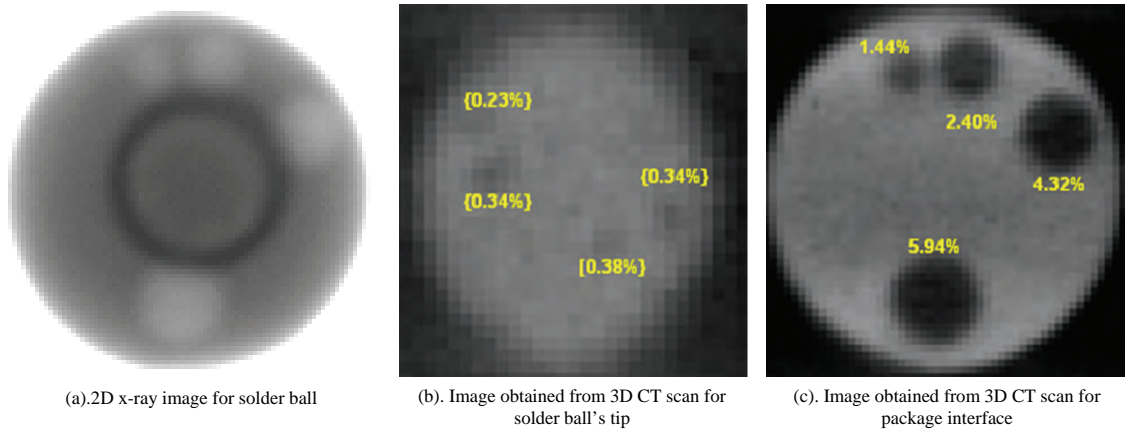


Fig. 9. 2D x-ray images versus 3D CT scan images.

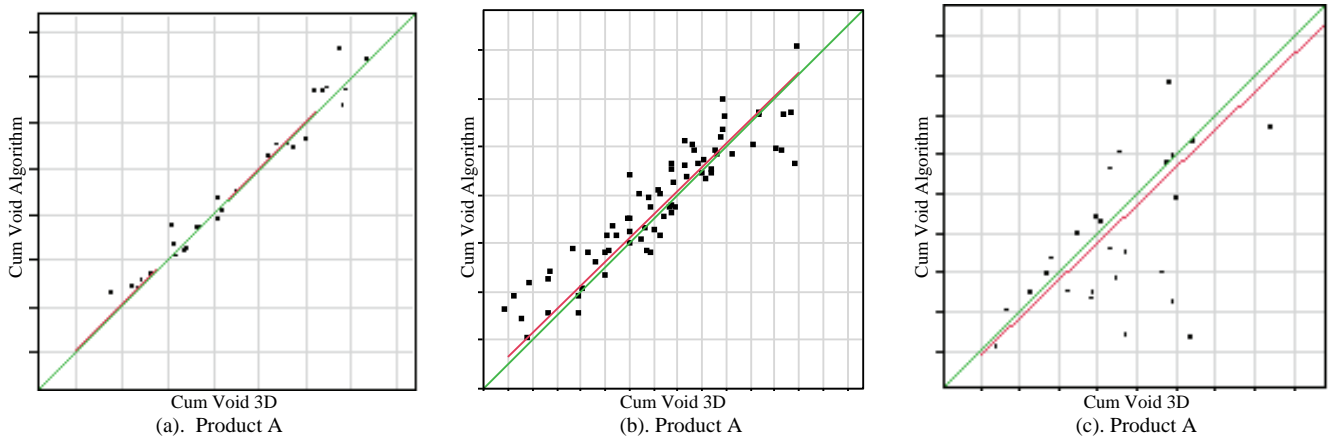


Fig. 10. 3D and Algorithm Cumulative Voiding Comparison

3.2. Comparison with the data obtained from 2D X-ray images by trained operator

Voids in many random balls in product lines A and B, were measured manually by trained operators. The operator takes 4 minutes to locate and measure one void in the ball. The operator locates and measures the void percentage by manually changing the 2D x-ray image intensity and contrast using an image processing program and then manually using a mouse to determine the extent of a void. The actual void percentage is the ratio of void area to the solder ball area. However the operator measures the void percentage by $(D_{av}/D_{solder\ joint})^2$ where $D_{solder\ joint}$ is the solder ball diameter and D_{av} is the average of void width (D_1) and void height (D_2) as illustrated in Fig. 8(a). The operator method is accurate if the void has a circular shape, but it is not accurate if the void has an irregular shape such as the one shown in Fig. 8(b). In this latter case, the operator method produces an error equal to 2.7% of the actual void percentage value. The data obtained by the trained operators was compared to the data obtained by the proposed algorithm. The proposed method results in a correlation squared value with the operator data of 96% and 93% for product lines A and B, respectively, with no significant bias. It should be noted that a correlation squared value greater than or equal to 75% with no significant bias corresponds to well correlated data.

3.3. Comparison with Data Obtained from 3D CT Scan by Trained Operator

Using 2D x-ray images does not give information regarding the void's depth within the ball. Furthermore, the use of the 2D images will produce inaccuracies in the case of overlapping voids. Using a 3D CT scan allows the operator to have 2D images at different layers (depths) of the solder ball which helps to see the isolated voids clearly without the interference of vias and die balls. Fig. 9(a) shows the 2D x-ray image where 4 visible voids around the via are present while Figs. 9(b) and (c) show the 3D CT scan images at the solder ball's tip and package interface, respectively. Figs. 9(b) and (c) show 8 different voids which are seen as 4 voids in the 2D x-ray image due to the via interference which occludes a portion of those voids. The trained operators measure the visible voids in the 3D CT scan images using a manual calculation which produces less error in this case due to the fact that the voids do not overlap and have circular shapes. Voids in many random balls in product lines A, B, and C were measured manually by the trained operators. The data obtained by the trained operator from

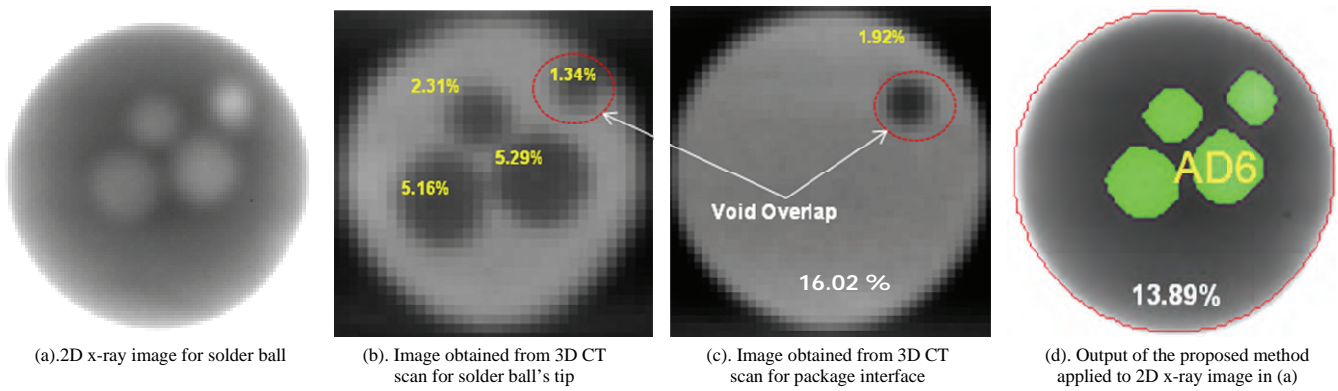


Fig. 11. Comparison between the results obtained by the proposed method from 2D x-ray images and the results obtained by trained operator from the 3D CT scan images.

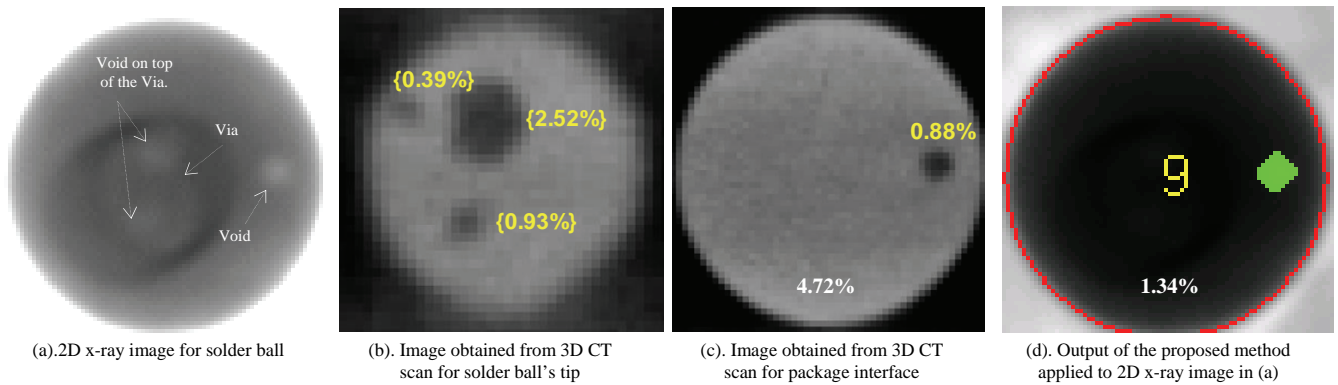


Fig. 12. Limitations of processing the 2D x-ray images.

the 3D CT scan images is used as ground truth and is used for comparison with data from the proposed algorithm applied to the 2D x-ray images. The proposed method results in a correlation squared with the ground truth data of 97%, 91%, and 77% for product lines A, B, and C, respectively, with no significant bias as shown in Figures 10(a), (b), and (c), respectively. It should be noted that, for product line C, balls with voids occurring on top of vias were excluded from the statistics.

The mismatch between results obtained from 2D x-ray images and the results obtained from 3D CT scan images is due to the missing information in the 2D x-ray image as compared to the 3D CT scan images, especially if there are overlaps or via interference in the image. These are the limitations of processing 2D x-ray images. The following examples show the limitations of the proposed method when applied to 2D x-ray images. Fig. 11(a) shows the 2D x-ray image where 4 voids can be seen clearly. Figs. 11(b) and (c) show the images from the 3D CT scan images at the solder ball's tip and package interface, respectively. Figs. 11(b) and (c) show 5 different voids where 2 voids at different depths overlap and are seen as one void in the 2D x-ray image. The result of the proposed method is shown in Fig. 11(d). It can be seen that the proposed algorithm detects all visible voids in the input 2D x-ray image of Fig. 11(a). The proposed method gives a total void percentage equal to 13.89% versus 16.02% from the 3D CT scan ground truth data. The error between the two different methods is 2.34% which is due to the overlapped voids and the human tolerance error of the operator. The proposed method detects the voids that are visible inside the 2D x-ray images and it cannot detect the overlapped void due to the limitations of the 2D x-ray image. Another example is given in Fig. 12 which illustrates the limitation of the 2D x-ray images when the voids lie on top of the via which makes it hard to segregate the voids from the via due to the similarities of the gray level values in both the voids and the vias.

Fig. 13 shows the comparison between the results obtained by the proposed algorithm and trained operators. Many trained operators were asked to calculate the void percentage for the largest void in an image manually for some random solder balls in product line C. The operators' results are compared with each other and show a 7% inconsistency. The result of two experienced engineers were averaged and given in Fig. 13 as "CNTRL". The result from the proposed algorithm ("Auto" in Fig. 13) compares well to the experienced engineer ("CNTRL" in Fig. 13). The proposed algorithm not only saves time, but also produces consistent results when compared to operators' results.

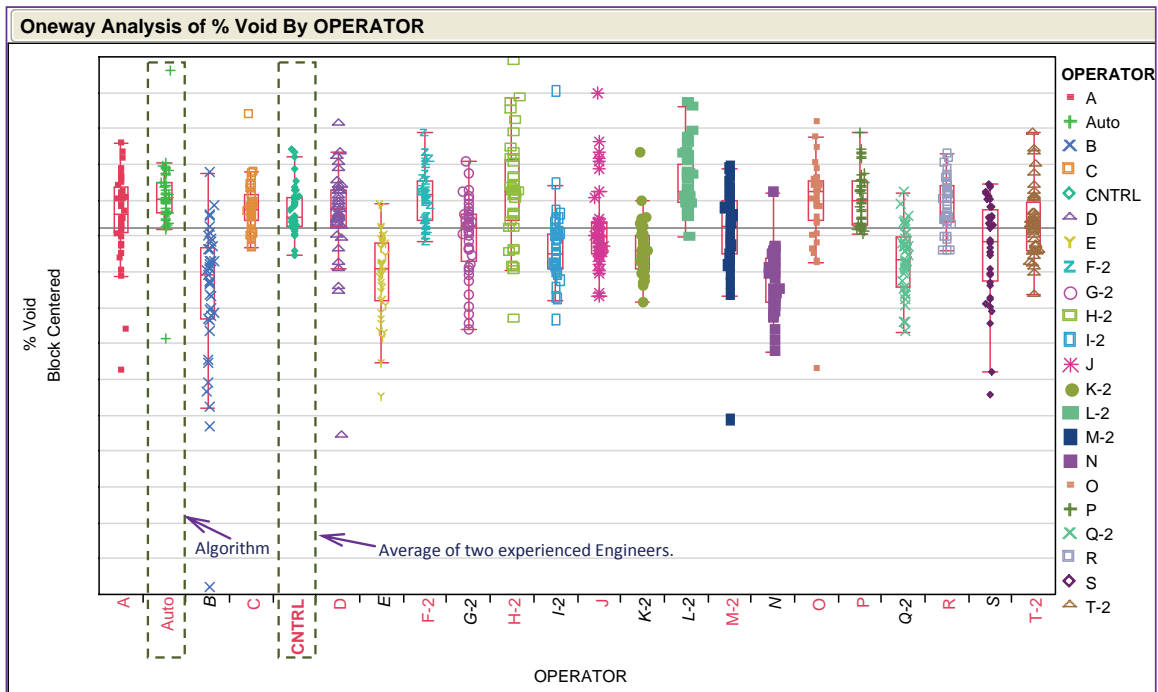


Fig. 13. Proposed algorithm (Auto) versus engineer: algorithm performance (Auto) compares well to the experienced engineer (CNTRL).

4. Conclusion

A robust automatic void detection scheme is presented in order to allow automated inspection and automated manufacturing quality assessment. The proposed method is fully automated and can benefit the manufacturing process by reducing operator effort and process variability. The method has been implemented in a standalone PC that is configured to receive images from a 2D x-ray system. The proposed method can enable compliance to IPCA610D for cumulative voiding of 25% or less in post SMT solder joints and the proposed JEDEC guideline in preparation by the JC-14-1 committee for cumulative voiding in a single solder ball not to exceed 15%.

5. References

- [1] R. Aspandiar, "Voids in Solder Joints," *Surface Mount Technology Association Journal*, vol. 19, Issue 4, pp28-36, 2006.
- [2] R. Prasad, "BGA Voids and Their Sources in SMT Assemblies," *Surface Mount Technology Magazine, SMT*, 2003.
- [3] Q. Yu, T. Shibutani, Y. Kobayashi, and M. Shiratori, "The effect of voids on thermal reliability of BGA lead free solder joint and reliability detecting standard," *Thermomechanical Phenomena in Electronic Systems -Proceedings of the Intersociety Conference*. pp. 1024-1030, San Diego, CA, United states, 2006.
- [4] V. Tvergaard, and Niordson, C., "Non-Local Plasticity Effect on Interaction of Different Size Voids," *Int. J. Plast.*, vol. 20, pp. 107-120.
- [5] R. M. Haralick, and Linda G. Shapiro, "Computer and Robot Vision," pp. 28-48: Addison-Wesley, 1992.
- [6] Rafael C. Gonzalez, and R. E. Woods, *Digital Image Processing*: Prentice Hall, 2003.
- [7] J. Canny, "A Computational Approach to Edge Detection," *IEEE Transactions on Pattern Analysis and Machine Intelligence*, vol. PAMI-8, no. 6, pp. 679-698, 1986.
- [8] J. S. Lim, "Two-Dimensional Signal and Image Processing," Englewood Cliffs, pp. 478-488., NJ: Prentice Hall, 1990.
- [9] J. R. Parker, "Algorithms for Image Processing and Computer Vision," pp. 23-29, New York: John Wiley & Sons, Inc., 1997.
- [10] S. Tabbone, "Detecting junctions using properties of the Laplacian of Gaussian detector," *Proceedings of the 12th IAPR International Conference on Pattern Recognition (Cat. No.94CH3440-5)*. pp. 52-6, Los Alamitos, CA, USA, 1994.
- [11] S. A. Tabbone, L. Alonso, and D. Ziou, "Behavior of the Laplacian of Gaussian extrema," *Journal of Mathematical Imaging and Vision*, vol. 23, no. 1, pp. 107-128, 2005.
- [12] <http://homepages.inf.ed.ac.uk/rbf/HIPR2/log.htm>.
- [13] B. Rein van den, and B. Richard van, "Methods for fast morphological image transforms using bitmapped binary images," *CVGIP: Graph. Models Image Process.*, vol. 54, no. 3, pp. 252-258, 1992.